JOURNAL OF THERMOPHYSICS AND HEAT TRANSFER
Vol. 8, No. 2, April–June 1994

# Refractive Index and Scattering Effects on Radiation in a Semitransparent Laminated Layer

C. M. Spuckler* and R. Siegel†
*NASA Lewis Research Center, Cleveland, Ohio 44135*

**Heat transfer characteristics are analyzed for a laminated layer of two semitransparent scattering materials with refractive indices larger than one. Each side of the composite is heated by radiation and convection. Energy is transferred internally by conduction, emission, absorption, and isotropic scattering. The external surfaces of the composite and its internal interface are diffuse, which is intended to model composite ceramics in high-temperature applications. The two sublayers can have differing refractive indices greater than one. This causes internal reflection of some energy within the layers. Coupled with scattering, this has a substantial effect on the temperature distribution. Results are given for various optical thicknesses and refractive indices of the sublayers, and for scattering albedos up to one. Comparisons of numerical solutions are made with limiting cases based on the pure scattering, radiative diffusion, transparent, and opaque limits in the individual layers. The limiting solutions are very useful because they are convenient to evaluate and provide accurate results for many cases of interest.**

## Nomenclature

$A_1, A_2, A_3, A_4$ = quantities defined in Eq. (10)
$a_j$ = absorption coefficient of $j$th layer, $m^{-1}$
$C_1, C_2, C_3, C_4$ = quantities defined in Eq. (11)
$D_1, D_2$ = the thicknesses of the two plane layers in Fig. 1, m
$E_1, E_2, E_3$ = exponential integral functions, $E_n(x) = \int_0^1 \mu^{n-2} \exp(-x/\mu)\, d\mu$
$F(n)$ = function of refractive index defined in Eq. (13)
$H_j$ = dimensionless convection-radiation parameter, $h_j/\sigma T_{g1}^3$
$h_1, h_2$ = convective heat transfer coefficients on two sides of laminated layer, $W/m^2 \cdot K$
$I_j$ = radiative source function in $j$th layer, $W/m^2$; $\bar{I}_j = \pi I_j/n_j^2 \sigma T_{g1}^4$
$K_j$ = extinction coefficient of $j$th layer, $a_j + \sigma_{sj}$, $m^{-1}$
$k_j$ = thermal conductivity of $j$th layer, $W/m \cdot K$
$N_j$ = conduction-radiation parameter, $k_j/\sigma T_{g1}^3 D_j$
$n_j$ = refractive index of $j$th layer
$q$ = heat flux, $W/m^2$; $\bar{q} = q/\sigma T_{g1}^4$
$q_a, q_b, q_c, q_d$ = radiative heat fluxes at interfaces, Fig. 1, $W/m^2$
$q_r^o$ = externally incident radiation flux, $W/m^2$; $\tilde{q}_r^o = q_r^o/\sigma T_{g1}^4$
$q_{rj}$ = radiative heat flux in $j$th layer, $W/m^2$; $\tilde{q}_{rj} = q_{rj}/\sigma T_{g1}^4$
$T$ = absolute temperature, K
$T_{g1}, T_{g2}$ = gas temperatures on two sides of laminated layer, K
$t$ = dimensionless temperature, $T/T_{g1}$
$X$ = $X_1$ in layer 1; $1 + X_2$ in layer 2
$x$ = coordinate through entire two-layer laminate
$x_j$ = coordinate in the $j$th layer, m; $X_j = x_j/D_j$
$\kappa$ = extinction coefficient in the complex index of refraction
$\kappa_j$ = optical coordinate in $j$th layer $K_j \cdot x_j$; $\kappa_{Dj}$, optical thickness, $K_j \cdot D_j$
$\lambda_0$ = wavelength of radiation in vacuum
$\rho$ = reflectivity of interface for internally incident radiation
$\sigma$ = Stefan-Boltzmann constant, $W/m^2 \cdot K^4$
$\sigma_{sj}$ = scattering coefficient of the $j$th layer, $m^{-1}$
$\Psi_1$ = dimensionless radiative heat flux defined after Eq. (20)
$\Omega_j$ = scattering albedo of the $j$th layer, $\sigma_{sj}/K_j$

*Subscripts*
$a, b, c, d$ = four internal sides of the interfaces in Fig. 1
$g$ = gas on either side of laminated layer
$H, S$ = higher and smaller refractive indices
$i, o$ = incoming and outgoing radiation
$j$ = index indicating 1st or 2nd layer
$r$ = radiative quantity
1, 2 = layers adjacent to the hotter and cooler surroundings, respectively; quantities in the hotter and cooler surroundings

*Superscript*
$o$ = quantity incident from the outside

## Introduction

CERAMIC parts and coatings are being developed for high-temperature applications. For strength, some ceramics have reinforcing layers or are laminated, so heat transfer in composite layers must be considered. The surrounding temperatures are high, giving significant heating by radiation and convection. Some ceramics are partly transparent, so their heat transfer behavior is influenced by internal radiative heat absorption, scattering, and emission. It must be determined when radiative processes can be important, and how large an

Received March 4, 1993; revision received June 21, 1993; accepted for publication June 23, 1993. 

*Research Scientist, Heat Transfer Branch, Internal Fluid Mechanics Division.
†Senior Research Scientist, Lewis Research Academy. Fellow AIAA.

effect they have compared with calculations for materials that are assumed opaque.

In a laminated layer the optical and thermal properties of each layer interact to affect the temperature distribution and heat transfer in the entire layer. The refractive indices of the layers can have a considerable effect. Surface reflections depend on the ratio of refractive indices across the interface; this affects the amount of external radiation transmitted into the composite and the amount reflected from internal interfaces. Coupled with this is the very significant effect that emission in a material depends on the square of its refractive index so that internal emission can be many times that of a blackbody radiating into a vacuum. To prevent radiation through an interface from exceeding that of a blackbody, there is energy reflection at the internal surface of an interface, mostly by total reflection. Scattering is another means for energy transfer in the layer, and it interacts with the internally reflected energy.

To predict heat treating and cooling of glass plates, Gardon[1] developed an analysis for temperature distributions in absorbing-emitting layers, including index of refraction effects. The interfaces are optically smooth, so reflections are specular and are computed from Fresnel reflection laws. A similar application[2] predicted heating of a window in a re-entry vehicle. Several recent papers[3-5] have further examined the effects of Fresnel boundary reflections and nonunity refractive index. In other instances, diffuse interfaces have been assumed in analyses of steady and transient heat transfer of single or multiple plane layers.[6-12] Spectral and directional effects at solid walls bounding a semitransparent layer are considered in Ref. 13. Directional variations of the emission-reflection characteristics of the bounding solid walls were found to have small effects. Thomas[14] set up a solution procedure to include a ceramic interface that is partially specular and diffuse.

To examine internal radiation effects in composite materials for high-temperature applications, a detailed analysis is required for a scattering composite subjected to radiation and convection on each outer surface. In the present analysis each layer emits, absorbs, and isotropically scatters radiation. The effect is examined of large scattering albedos and a different refractive index in each layer. The outer surfaces and the interface between the two layers are assumed diffuse to approximate behavior for ceramics that have not been polished and are bonded together. When transmitted or internally emitted radiation reaches the inner surface of an interface, the radiation is assumed diffuse. Total reflection occurs for a portion of the radiant energy if the material is adjacent to one of lower refractive index.

This analysis continues the investigations in Refs. 8–10 and 12. The results in Refs. 8 and 9 are for single layers; the interaction between two layers with considerably different properties is examined here. The coupling conditions across the internal interface are developed for two or multiple layers. In conjunction with appropriate interface conditions, the governing integral equations for energy transfer are solved numerically. References 10 and 12 are for the special case of radiation only. They showed how the solution could be obtained analytically for multiple layers with refractive indices greater than one, by using the solution for a single layer with a refractive index of one along with interface coupling conditions. The present results include conduction and convection, and reduce to those in Ref. 12 when radiation is dominating.

Solutions for important limiting cases are developed here. They provide insight into the behavior of the results, and are useful for making quick estimates of radiation effects. Limiting cases are for pure scattering in one layer, radiative diffusion in one or both layers, and one or both layers either transparent or opaque. For pure scattering, there is partial transmission of incident radiation through one layer to reach the second layer, but temperature is affected only by conduction within the pure scattering layer.

## Analysis

The laminated plane layer is made of two different ceramic materials with thicknesses $D_1$ and $D_2$ (Fig. 1). Each layer absorbs, emits, and isotropically scatters radiation. The layers have absorption and scattering coefficients $a_1$, $\sigma_{s1}$ and $a_2$, $\sigma_{s2}$. The local optical depth in each layer is related to its individual $x_j$ coordinate by $\kappa_j = (a_j + \sigma_{sj})x_j$, where $j = 1, 2$. There is diffuse radiation $q^o_{r1}$ and $q^o_{r2}$ incident from the surroundings on the two outer boundaries $x_1 = 0$ and $x_2 = D_2$. Inside each layer there are outgoing and incoming fluxes, $q_o$ and $q_i$, at each interface. External convective heat transfer is provided by external gas flows at $T_{g1}$ and $T_{g2}$ with $h_1$ and $h_2$. For convenience, $q^o_{r1} > q^o_{r2}$ and $T_{g1} > T_{g2}$ in the present study. Each material has a constant $n_j > 1$. The ceramic material surfaces are assumed sufficiently rough, so the interface between the two ceramic layers and the two exterior surfaces are all assumed diffuse.

### Temperature Distribution Relations from Energy Equation

Within each layer, energy is transferred by conduction and radiation according to the energy equation (Ref. 15, p. 695)

$$k_j \frac{d^2T_j}{dx_j^2} - \frac{dq_{rj}}{dx_j} = 0 \qquad (j = 1, 2) \tag{1}$$

Since the energy flux by combined radiation and conduction through the composite is a constant, Eq. (1) can be integrated with respect to $x$ and then equated to its values at $x_1 = 0$ and $x_2 = D_2$ to evaluate the constant of integration; this gives

$$k_1 \left.\frac{dT_1}{dx_1}\right|_{x1} - q_{r1}(x_1) = k_2 \left.\frac{dT_2}{dx_2}\right|_{x2} - q_{r2}(x_2) = k_1 \left.\frac{dT_1}{dx_1}\right|_0$$

$$- q_{r1}(x_1 = 0) = k_2 \left.\frac{dT_2}{dx_2}\right|_{D2} - q_{r2}(x_2 = D_2) \tag{2}$$

After partial reflection at the outer boundary, the incident radiation passes into the composite layer and interacts internally. There is no absorption at the exact plane of an outer boundary since an interface does not have any volume. Therefore, the conduction derivative terms at the boundaries in Eq.

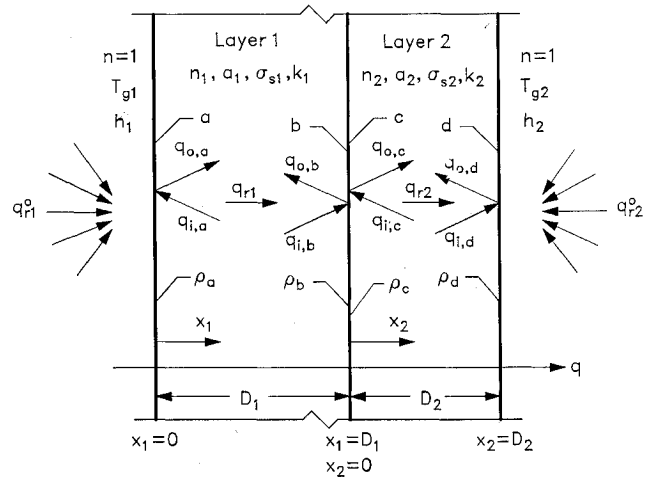


**Fig. 1 Geometry, coordinate system, and nomenclature for radiative fluxes for absorbing and scattering layer consisting of two sublayers with differing properties.**

(2) are equal to only the external convection, and Eq. (2) can be written as

$$-k_1 \left.\frac{dT_1}{dx_1}\right|_{x1} + q_{r1}(x_1) = h_1[T_{g1} - T_1(0)] + q_{r1}(x_1 = 0)$$
$$= h_2[T_2(D_2) - T_{g2}] + q_{r2}(x_2 = D_2)$$
$$= -k_2 \left.\frac{dT_2}{dx_2}\right|_{x2} + q_{r2}(x_2) \quad (3)$$

Equation (3) is integrated to give the following relations for the layer temperature distributions:

$$T_1(x_1) = T_1(x_1 = 0) - \frac{h_1}{k_1}[T_{g1} - T_1(x_1 = 0)]x_1 - \frac{x_1}{k_1} q_{r1}(x_1 = 0) + \frac{1}{k_1}\int_0^{x1} q_{r1}(x_1^*)\, dx_1^* \quad (4a)$$

$$T_2(x_2) = T_2(x_2 = 0) - \frac{h_2}{k_2}[T_2(x_2 = D_2) - T_{g2}]x_2 - \frac{x_2}{k_2} q_{r2}(x_2 = D_2) + \frac{1}{k_2}\int_0^{x2} q_{r2}(x_2^*)\, dx_2^* \quad (4b)$$

Equations (4a) and (4b) are evaluated respectively at the boundaries $x_1 = D_1$ and $x_2 = D_2$, and the overall temperature difference for the composite, $T_1(x_1 = 0) - T_2(x_2 = D_2)$, is found by addition noting that at the internal interface, $T_1(x_1 = D_1) = T_2(x_2 = 0)$. Then, by using the equality of the two central sets of terms in Eq. (3), the $T_2(x_2 = D_2)$ or $T_1(x_1 = 0)$ can be eliminated to yield the two surface temperatures in the form

$$T_1(x_1 = 0) = T_{g1} + \left[1 + \frac{h_1}{h_2} + h_1\left(\frac{D_1}{k_1} + \frac{D_2}{k_2}\right)\right]^{-1} \times \left[T_{g2} - T_{g1} + \left(\frac{1}{h_2} + \frac{D_1}{k_1} + \frac{D_2}{k_2}\right) q_{r1}(0) - \frac{1}{h_2} q_{r2}(D_2) - \frac{1}{k_1}\int_0^{D1} q_{r1}(x_1)\, dx_1 - \frac{1}{k_2}\int_0^{D2} q_{r2}(x_2)\, dx_2\right] \quad (5a)$$

$$T_2(x_2 = D_2) = T_{g2} - \left[1 + \frac{h_2}{h_1} + h_2\left(\frac{D_1}{k_1} + \frac{D_2}{k_2}\right)\right]^{-1} \times \left[T_{g2} - T_{g1} + \left(\frac{1}{h_1} + \frac{D_1}{k_1} + \frac{D_2}{k_2}\right) q_{r2}(D_2) - \frac{1}{h_1} q_{r1}(0) - \frac{1}{k_1}\int_0^{D1} q_{r1}(x_1)\, dx_1 - \frac{1}{k_2}\int_0^{D2} q_{r2}(x_2)\, dx_2\right] \quad (5b)$$

**Relations for Radiative Flux**

Equations (4) and (5) for the temperature distributions contain the radiative flux, $q_{rj}(x_j)$, where $j = 1, 2$. In a scattering medium the radiative flux depends on the unknown radiative source function $I_j(x_j)$, and is given in each layer by (Ref. 15, p. 708)

$$q_{rj}(x_j) = 2q_o(x_j = 0)E_3(K_j x_j) - 2q_o(x_j = D_j)E_3[K_j(D_j - x_j)] + 2\pi K_j\left\{\int_0^{xj} I_j(x_j^*)E_2[K_j(x_j - x_j^*)]\, dx_j^* - \int_{xj}^{Dj} I_j(x_j^*)E_2[K_j(x_j^* - x_j)]\, dx_j^*\right\} \quad (6)$$

Equation (6) contains the diffuse fluxes $q_o(x_j = 0)$ and $q_o(x_j = D_j)$, leaving the internal surface of each layer boundary (Fig. 1). These fluxes are now expressed in terms of the fluxes incident from outside of each layer to provide coupling with the external radiative conditions, and with the energy coming across the internal interface.

By using the procedure in Ref. 12, a relation for outgoing flux is written at each diffuse interface in terms of transmitted and reflected energy fluxes (see nomenclature in Fig. 1):

$$q_{o,a} = q_{r1}^o n_1^2(1 - \rho_a) + q_{i,a}\rho_a \quad (7a)$$

$$q_{o,b} = q_{i,c}(n_1/n_2)^2(1 - \rho_b) + q_{i,b}\rho_b \quad (7b)$$

$$q_{o,d} = q_{r2}^o n_2^2(1 - \rho_d) + q_{i,d}\rho_d \quad (7c)$$

Since there are four internal interfaces, another independent relation is needed. This is obtained from continuity of radiative flux across the internal interface which gives

$$q_{i,b} - q_{o,b} = q_{o,c} - q_{i,c} \quad (7d)$$

As described in Ref. 12, by using $q_{rj}(x_j = 0) = q_o - q_i$ at interfaces $a$ and $c$, and $q_{rj}(x_j = D_j) = q_i - q_o$ at interfaces $b$ and $d$, Eq. (6) is used to obtain the internal incoming fluxes at the four internal boundaries as

$$q_{i,a} = 2q_{o,b}E_3(K_1D_1) + 2\pi K_1\int_0^{D1} I_1(x_1)E_2(K_1x_1)\, dx_1 \quad (8a)$$

$$q_{i,b} = 2q_{o,a}E_3(K_1D_1) + 2\pi K_1\int_0^{D1} I_1(x_1)E_2[K_1(D_1 - x_1)]\, dx_1 \quad (8b)$$

$$q_{i,c} = 2q_{o,d}E_3(K_2D_2) + 2\pi K_2\int_0^{D2} I_2(x_2)E_2(K_2x_2)\, dx_2 \quad (8c)$$

$$q_{i,d} = 2q_{o,c}E_3(K_2D_2) + 2\pi K_2\int_0^{D2} I_2(x_2)E_2[K_2(D_2 - x_2)]\, dx_2 \quad (8d)$$

The $q_i$ are now eliminated between Eqs. (7) and (8). The resulting simultaneous equations are solved for $q_o$ at each internal boundary to yield

$$q_{o,b} = \frac{\left(1 - \frac{A_4^2}{\rho_d}\right)(A_2C_3 + A_3C_1 + C_2) + A_2A_4\left(\frac{A_1C_1}{\rho_a} + \frac{A_4C_3}{\rho_d} + C_4\right)}{\left(1 - \frac{A_4^2}{\rho_d}\right)(1 - A_1A_3) + A_2A_4\left(1 - \frac{A_1^2}{\rho_a}\right)} \quad (9a)$$

$$q_{o,a} = C_1 + A_1q_{o,b} \quad (9b)$$

$$q_{o,c} = \frac{-\left(1 - \frac{A_1^2}{\rho_a}\right)(A_2C_3 + A_3C_1 + C_2) + (1 - A_1A_3)\left(\frac{A_1C_1}{\rho_a} + \frac{A_4C_3}{\rho_d} + C_4\right)}{\left(1 - \frac{A_4^2}{\rho_d}\right)(1 - A_1A_3) + A_2A_4\left(1 - \frac{A_1^2}{\rho_a}\right)} \tag{9c}$$

$$q_{o,d} = C_3 + A_4q_{o,c} \tag{9d}$$

where

$$A_1 \equiv 2\rho_aE_3(K_1D_1) \tag{10a}$$

$$A_2 \equiv 2(1 - \rho_b)(n_1/n_2)^2E_3(K_2D_2) \tag{10b}$$

$$A_3 \equiv 2\rho_bE_3(K_1D_1) \tag{10c}$$

$$A_4 \equiv 2\rho_dE_3(K_2D_2) \tag{10d}$$

$$C_1 \equiv (1 - \rho_a)n_1^2q_{r1}^o + 2\rho_a\pi K_1\int_0^{D_1} I_1(x_1)E_2(K_1x_1)\,dx_1 \tag{11a}$$

$$C_2 \equiv 2\pi\left\{(1 - \rho_b)\left(\frac{n_1}{n_2}\right)^2 K_2\int_0^{D_2} I_2(x_2)E_2(K_2x_2)\,dx_2 + \rho_bK_1\int_0^{D_1} I_1(x_1)E_2[K_1(D_1 - x_1)]\,dx_1\right\} \tag{11b}$$

$$C_3 \equiv (1 - \rho_d)n_2^2q_{r2}^o + 2\rho_d\pi K_2\int_0^{D_2} I_2(x_2)E_2[K_2(D_2 - x_2)]\,dx_2 \tag{11c}$$

$$C_4 \equiv 2\pi\left\{K_1\int_0^{D_1} I_1(x_1)E_2[K_1(D_1 - x_1)]\,dx_1 + K_2\int_0^{D_2} I_2(x_2)E_2(K_2x_2)\,dx_2\right\} \tag{11d}$$

**Equation for the Source Function**

The source function $I_j(x_j)$ required for the radiative flux is obtained in each layer from an integral equation (Ref. 15, p. 708)

$$I_j(x_j) = (1 - \Omega_j)n_j^2\frac{\sigma T_j^4(x_j)}{\pi} + \frac{\Omega_j}{2}\left\{\frac{q_o(x_j = 0)}{\pi}E_2(K_jx_j) + \frac{q_o(x_j = D_j)}{\pi}E_2[K_j(D_j - x_j)] + K_j\int_0^{D_j} I_j(x_j^*)E_1(K_j|x_j - x_j^*|)\,dx_j^*\right\} \quad (j = 1, 2) \tag{12}$$

**Solution Procedure**

An iterative solution is obtained by first assuming temperature and source function distributions in both layers. The $A_1$ to $A_4$ and $C_1$ to $C_4$ are evaluated from Eqs. (10) and (11) and are used to calculate the four $q_o$ from Eq. (9). New $I_1(x_1)$ and $I_2(x_2)$ are obtained by iterating Eq. (12), using the assumed $T_1(x_1)$ and $T_2(x_2)$. The flux distributions $q_{r1}(x_1)$ and $q_{r2}(x_2)$ are then evaluated from Eq. (6). New boundary temperatures $T_1(x_1 = 0)$ and $T_2(x_2 = D_2)$ are calculated from Eq. (5), and new temperature distributions $T_1(x_1)$ and $T_2(x_2)$ from Eq. (4). The new $T_1(x_1)$ and $T_2(x_2)$ and $I_1(x_1)$ and $I_2(x_2)$ are used to start a new iteration. The process is continued until a converged solution is obtained. For the numerical solution, the equations were placed in terms of the dimensionless variables and parameters defined in the nomenclature.

**Relations for Diffuse Interface Transmittance and Reflectance**

For diffuse interfaces, the roughness influences the transmission of radiation incident from the outside, and the reflection of radiation incident from within the layer. When the refractive index of the medium is greater than unity, the internal reflectivity must account for part of the internal radiation being totally reflected at the interface.

In the absence of other information, the interface characteristics were modeled by using integrated averages of the Fresnel reflection relations. For diffuse incident radiation, this gives (Ref. 15, p. 115)

$$\rho(n) \equiv F(n) = \frac{1}{2} + \frac{(3n + 1)(n - 1)}{6(n + 1)^2} + \frac{n^2(n^2 - 1)^2}{(n^2 + 1)^3}\ln\left(\frac{n - 1}{n + 1}\right) - \frac{2n^3(n^2 + 2n - 1)}{(n^2 + 1)(n^4 - 1)} + \frac{8n^4(n^4 + 1)}{(n^2 + 1)(n^4 - 1)^2}\ln(n) \qquad (n = n_H/n_S) \tag{13}$$

Equation (13) is for reflection from a material of higher refractive index where $n_H$ and $n_S$ are the "higher" and "smaller" $n$ values. Using Eq. (13) assumes the interface properties can be calculated by considering the media to be nonattenuating dielectrics, neglecting the effect of the extinction coefficient in the complex index of refraction. This is reasonable unless the extinction coefficient is large.[16] The $a$ in a material is related to its $\kappa$ (not to be confused with its optical thickness), by $a = 4\pi\kappa/\lambda_0$. Since wavelengths for thermal radiation are in the micrometer range, only a small value of $\kappa$ is required to provide a large value of $a$. If $\kappa$ is large enough to influence the interface reflectivity relations, $a$ is so large that the radiating layer is essentially opaque, unless its thickness is much smaller than the ceramic layers considered here. After allowing for energy incident at angles larger than the critical angle for total reflection, the $\rho(n)$ for diffuse radiation going in the direction from a higher to a smaller refractive index is found from[17]

$$\rho(n) = 1 - (1/n^2)[1 - F(n)] \qquad (n = n_H/n_S) \tag{14}$$

Values of $\rho(n)$ are in table 1 of Ref. 8 for various $n$. As $n$ increases, the amount of internal reflection becomes quite large.

**Numerical Solution Method**

The numerical solution of Eq. (12) for $I_j(x_j)$ in each layer requires integrating $I_j(x_j)$ multiplied by $E_1$. Since there is a singularity where $E_1(0) \to \infty$, the integrals were evaluated analytically for a small region where $x_j^*$ is near $x_j$ by using $I_j(x_j^*) \approx I_j(x_j)$, which is then taken out of the integral; the integration of $E_1$ with respect to $x_j^*$ is then done analytically. The integral away from the singularity was evaluated with the Gaussian integration subroutine QDAGS from the IMSL library. Each layer was divided into 21 evenly spaced grid points. For an optical thickness of 100 in one or both layers, some calculations were checked using 41 points in each layer, and the temperatures changed less than 1%. The $I_j(x_j)$ and $T_j^4(x_j)$ distributions were fitted during each iteration with the cubic spline subroutine CSINT from the IMSL library. The

Gaussian subroutine called for values of the integrand at unevenly spaced grid points, and during the calculations the required function values were interpolated from the spline fits.

**Diffusion and Opaque Approximations for Optically Thick Layers**

When the layer optical thickness is large, the limits of radiative diffusion or being opaque are of interest for comparison with the numerical solutions. Heat conduction combined with radiative diffusion gives a differential energy equation for each layer (Ref. 15, p. 837)

$$k_j \frac{d^2T_j}{dx_j^2} + \frac{d}{dx_j}\left(\frac{16\sigma n_j^2 T_j^3}{3K_j}\frac{dT_j}{dx_j}\right) = 0 \qquad (j = 1, 2) \quad (15)$$

The integral of Eq. (15) yields the negative of the heat flux by conduction and radiative diffusion through the layer. This is constant through the entire composite, so for either layer

$$\left(k_j + \frac{16\sigma n_j^2 T_j^3}{3K_j}\right)\frac{dT_j}{dx_j} = -q \qquad (j = 1, 2) \quad (16)$$

Integrating again gives for the temperature distribution in each layer

$$k_j T_j(x_j) + \frac{4\sigma n_j^2 T_j^4(x_j)}{3K_j} = -qx_j + \mathrm{CON}_j \qquad (j = 1, 2) \quad (17)$$

where CON is a constant of integration. Equation (17) is evaluated at the outer boundary of each layer ($x_1 = 0$, and $x_2 = D_2$); this gives an expression to eliminate the $\mathrm{CON}_j$ for each layer. To join the two layers, a continuous temperature is assumed at the internal interface. The temperature jump that occurs in some instances when using the diffusion approximation is neglected at the boundaries. The jump is small when the layers are optically thick and when conduction is comparable to radiation.[18] The convective and radiative balance at each outside boundary, and the conduction/radiative diffusion relation, Eq. (17), in each layer provide the following dimensionless equations that are solved for the two external boundary temperatures, the internal interface temperature, and the heat flow through the composite layer:

$$H_1[1 - t_1(0)] + (1 - \rho_a)n_1^2[\tilde{q}_{r1}^o - t_1^4(0)] - \tilde{q} = 0 \quad (18a)$$

$$N_1[t_1(0) - t_1(1)] + \frac{4n_1^2}{3\kappa_{D1}}[t_1^4(0) - t_1^4(1)] - \tilde{q} = 0 \quad (18b)$$

$$N_2[t_2(0) - t_2(1)] + \frac{4n_2^2}{3\kappa_{D2}}[t_2^4(0) - t_2^4(1)] - \tilde{q} = 0 \quad (18c)$$

$$H_2[t_2(1) - t_{g2}] + (1 - \rho_d)n_2^2[t_2^4(1) - \tilde{q}_{r2}^o] - \tilde{q} = 0 \quad (18d)$$

In the limit when one or both layers are opaque, the solution is obtained by letting the $\kappa_{D1}$ and/or $\kappa_{D2}$ be very large in Eq. (18).

**Pure Scattering or Transparent Layer Combined with an Optically Thick Layer**

Another useful limit is to have a highly scattering layer bonded to an optically thick layer: this helps characterize a scattering coating on an opaque substrate. A very convenient solution for this special case is now developed. In the limit when $\Omega_1 = 1$, Eq. (12) becomes

$$\pi I_1(\kappa_1) = \frac{1}{2}[q_{o,a}E_2(\kappa_1) + q_{o,b}E_2(\kappa_{D1} - \kappa_1)] + \frac{1}{2}\int_0^{\kappa_{D1}} \pi I_1(\kappa_1^*)E_1(|\kappa_1 - \kappa_1^*|)\, d\kappa_1^* \quad (19)$$

In this limit there is no absorption in the first layer, so radiation does not affect the temperature distribution established by heat conduction. The radiative heat flux is constant through the layer and is found by evaluating Eq. (6) at $x_1 = 0$

$$q_{r1} = q_{o,a} - 2q_{o,b}E_3(\kappa_{D1}) - 2\pi\int_0^{\kappa_{D1}} I_1(\kappa_1)E_2(\kappa_1)\, d\kappa_1 \quad (20)$$

It is now noted that Eqs. (19) and (20) are identical in form to Eqs. (1) and (2) in Ref. 10. Then $q_{r1}/(q_{o,a} - q_{o,b}) \equiv \Psi_1$ has the same values as given in Ref. 10 (also see Ref. 19). The technique developed in Ref. 10 can be used to find $q_{r1}$ through the pure scattering layer. In Ref. 10 the layer has $n > 1$, but is surrounded by a medium with $n = 1$. Here, the layer has one side bounded by a medium with $n > 1$. Incorporating this change into the analytical method gives the radiative heat flux through the pure scattering layer as

$$\frac{q_r}{q_{r1}^o - \sigma T_1^4(D_1)} = \frac{\Psi_1 n_1^2}{1 + \Psi_1\left(\frac{\rho_a}{1 - \rho_a} + \frac{\rho_b}{1 - \rho_b}\right)} \quad (21)$$

This is added to the heat flux independently transferred through the first layer by conduction. At the internal interface the second layer receives energy by radiation and conduction, and energy is transferred within this optically thick layer by radiative diffusion and conduction. Then, in a similar way to Eq. (18), the two outer boundary temperatures, the internal interface temperature, and the heat flux through the composite are obtained by solving

$$H_1[1 - t_1(0)] - N_1[t_1(0) - t_1(1)] = 0 \quad (22a)$$

$$\frac{1 - t_1(1)}{\frac{1}{H_1} + \frac{1}{N_1}} + \frac{n_1^2\Psi_1}{1 + \Psi_1\left(\frac{\rho_a}{1 - \rho_a} + \frac{\rho_b}{1 - \rho_b}\right)} \times [\tilde{q}_{r1}^o - t_1^4(1)] - \tilde{q} = 0 \quad (22b)$$

$$N_2[t_2(0) - t_2(1)] + \frac{4n_2^2}{3\kappa_{D2}}[t_2^4(0) - t_2^4(1)] - \tilde{q} = 0 \quad (22c)$$

$$H_2[t_2(1) - t_{g2}] + (1 - \rho_d)n_2^2[t_2^4(1) - \tilde{q}_{r2}^o] - \tilde{q} = 0 \quad (22d)$$

The $t_2(X_2)$ in the optically thick layer is found from Eq. (17).

When there is no scattering and no absorption in the first layer, $q_{r1} = q_{o,a} - q_{o,b}$ and $\Psi_1 = 1$. Equation (22) then provides results for a completely transparent heat conducting layer laminated to an optically thick layer.

## Results and Discussion

Temperature distributions and heat fluxes are now presented to demonstrate important characteristics of radiative heat transfer in a two-layer laminated region. Iterative numerical solution results are compared with limiting cases. The limiting solutions are very useful for some conditions of important practical interest, and are convenient to evaluate.

Figure 2 illustrates the connection of the present work to results in a previous paper,[12] where the analytical solution was obtained for the temperature distribution and radiative transfer in a two-layer composite in the limit of negligible heat conduction and external convection. Since that limit is readily evaluated from convenient analytical expressions, it is worth demonstrating that it gives correct results and is useful for predicting behavior of absorbing and scattering media when $N_j$ and $H_j$ are small. For Fig. 2 the layers have refractive indices $n_1 = 1.5$ and $n_2 = 3.0$, and optical thicknesses $\kappa_{D1} = 3$ and $\kappa_{D2} = 30$. The pure radiation solution for the temper-

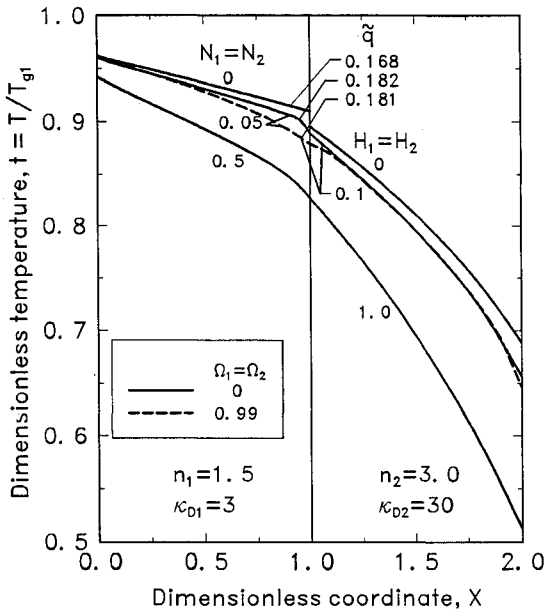


**Fig. 2 Comparisons of computed results without scattering, and with high scattering, and including conduction and convection, with results for the limiting solution for radiation only.**

ature distribution, as given by the uppermost curves, is closely approached by the present results when $N_1 = N_2 < 0.05$, and $H_1 = H_2 < 0.1$. Agreement is shown for no scattering in both layers, $\Omega_1 = \Omega_2 = 0$ (solid line), and for high scattering, $\Omega_1 = \Omega_2 = 0.99$ (dashed line). The pure radiation solution has a temperature jump at the internal interface. For absorption only, the numerical solution exhibits this trend by having a higher temperature gradient near the internal interface; when scattering is large, the temperature variation is diffused and the distribution becomes smooth across the interface.

Temperature distributions were obtained in Ref. 8 in a single absorbing layer with $n > 1$, and for the same boundary conditions as in the present analysis. Figure 3 shows the contrast between temperature distributions in a single layer with $n_1 = n_2 = 1.5$ throughout (dot-dash lines), and a two-layer composite (solid lines) with a larger refractive index in the second layer, $n_1 = 1.5$ and $n_2 = 3.0$. The two layers have equal thermal conductivities and equal optical thicknesses. The results are for absorption only; scattering is examined later. The effect of $n_1 \neq n_2$ is shown as a function of optical thickness which, for both layers combined, varies from $\kappa_{D1} + \kappa_{D2} = \kappa_D = 0.02$–$20$. Limits are shown for a transparent composite $\kappa_D = 0$ (short dash line) computed for heat conduction in a layer with convection at the boundaries, and for an opaque composite $\kappa_D = \infty$ (long dash line) computed from Eq. (18). For an intermediate range of optical thicknesses near $\kappa_{D1} = \kappa_{D2} = 1$, where radiation is most significant, an increased $n_2$ value tends to make temperatures in the second layer more uniform. For $\kappa_D < 1$, a larger $n_2$ increases the temperatures in both layers as a result of greater retention of energy in the second layer by total reflections. For $\kappa_D = 10$ the second layer temperatures become more uniform causing the first layer temperatures to decrease. For small and large $\kappa_D$, the solution approaches the transparent and opaque limits. At these limits, energy transfer within the layers is by conduction (the opaque limit has radiation absorption and emission only at the outer surfaces).

To show effects of scattering, Fig. 4 compares results from Fig. 3 (solid curves) with temperature distributions for a high scattering albedo in the first layer (dashed curves). The $\Omega_1 = 0.999$, while the second layer has no scattering, $\Omega_2 = 0$. For large scattering, and therefore, small absorption and emission, heat transport in the first layer is mainly by conduction so its temperature profile becomes linear. Radiative energy is scattered through the first layer and absorbed in the second. Since radiative penetration through the first layer depends on $\kappa_{D1}$, the change from low to high $\Omega_1$, while keeping $\kappa_{D1}$ the same, had little effect on the second layer temperature distribution. For the largest optical thickness in the second layer, $\kappa_{D2} = 10$, the dotted curve shows the comparison of pure scattering in the first layer ($\Omega_1 = 1$), with radiation diffusion and heat conduction in the second. This solution, which is

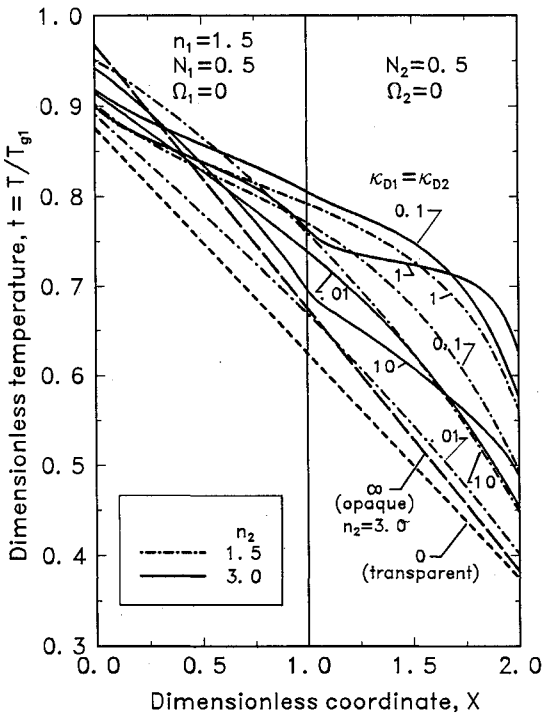


**Fig. 3 Effect of having different refractive indices in the two layers of the composite for optical thicknesses ranging from thin to thick, and comparisons with transparent and opaque approximations; $t_{s1} = t_{g1} = 1$, $t_{s2} = t_{g2} = 0.25$, $H_1 = H_2 = 1$.**

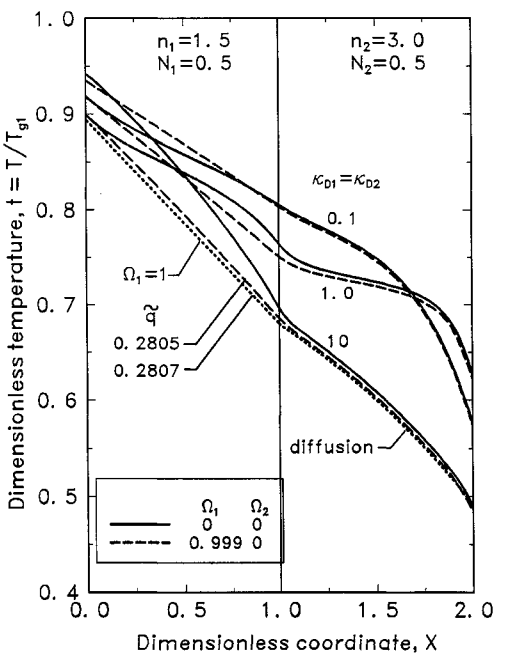


**Fig. 4 Effect of large scattering in the first layer for two layers with different refractive indices, and comparison with the approximation of pure scattering in the first layer and diffusion in the second layer; $t_{s1} = t_{g1} = 1$, $t_{s2} = t_{g2} = 0.25$, $H_1 = H_2 = 1$.**

readily evaluated from Eq. (22), provides very good results for both the temperature distribution and heat flux. It can be very helpful for evaluating the effect of large scattering in a layer bonded to an optically thick substrate.

The solid curves in Fig. 5a are for the same $n_1 = 1.5$ and $n_2 = 3.0$ in Fig. 3, and a comparison is made for $n = 1.5$ in both layers (dot-dash curves). The $N_1 = N_2 = 0.5$ are the same as in Fig. 3, but the $\kappa_{D1}$ and $\kappa_{D2}$ are now unequal. The first layer has $\kappa_{D1} = 1$, which is an intermediate value that provides a significant radiation effect on the temperature distribution; the second layer has $\kappa_{D2} = 0.01-100$. Having $n_2 > n_1$ tends to equalize the temperature in the second layer when its optical thickness is near $\kappa_{D2} = 1$, so it yields a significant radiation effect since it is not too optically thin or thick. Results for absorption only (solid curves) are compared with those for high scattering in the first layer, $\Omega_1 = 0.99$ (dashed curves), and no scattering ($\Omega_2 = 0$) in the second layer which is either optically thin ($\kappa_{D2} = 0.01$) or thick ($\kappa_{D2} = 100$). When $\Omega_1 = 0.99$ (dashed curves) absorption in the first layer is small, $a_1 D_1 = 0.01$, so its temperature profile is dominated by heat conduction and is linear. For high $\Omega_1$, decreased absorption in the first layer yields lower temperatures in the second layer than when $\Omega_1 = 0$.

The optical thicknesses of the layers are reversed in Fig. 5b with the other parameters the same as in Fig. 5a. The second layer has $\kappa_{D2} = 1.0$, while the first layer varies from $\kappa_{D1} = 0.01$ to 100. A large $\kappa_{D1}$ produces a large temperature decrease in the first layer, giving reduced temperatures in the second layer. When $\kappa_{D1}$ is small, the temperature distribution depends primarily on heat conduction and is nearly linear. For $n_2 = 3$, the temperature profiles become more uniform in the central portion of the second layer as a result of increased internal reflections.

In Fig. 6a, $\kappa_{D2}$ is made large, $\kappa_{D2} = 100$, to simulate an opaque substrate. The same parameters are retained as in Fig. 5b, and $\kappa_{D1}$ varies from 0.01 to 100. The temperature profiles in each layer are nearly linear and the temperature at the internal interface decreases with increasing $\kappa_{D1}$. For small and large $\kappa_{D1}$, the results approach the transparent-

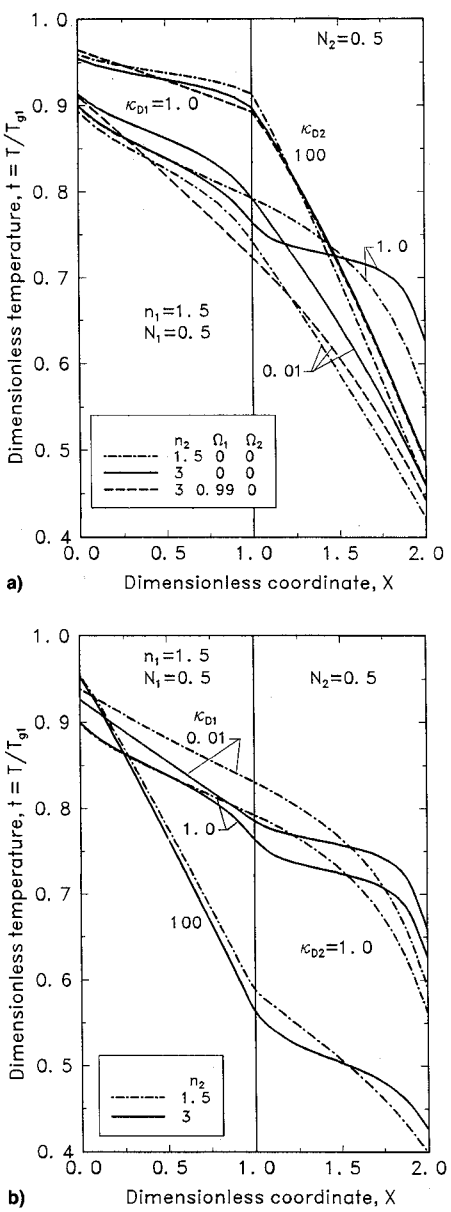


Fig. 5 Effect on temperature distributions of different optical thicknesses in the two layers of the composite; $t_{s1} = t_{g1} = 1$, $t_{s2} = t_{g2} = 0.25$, $H_1 = H_2 = 1$: a) $\kappa_{D1} = 1$, $\kappa_{D2} = 0.01-100$, and comparisons are made for high scattering in the first layer and b) $\kappa_{D1} = 0.01-100$, $\kappa_{D2} = 1$.

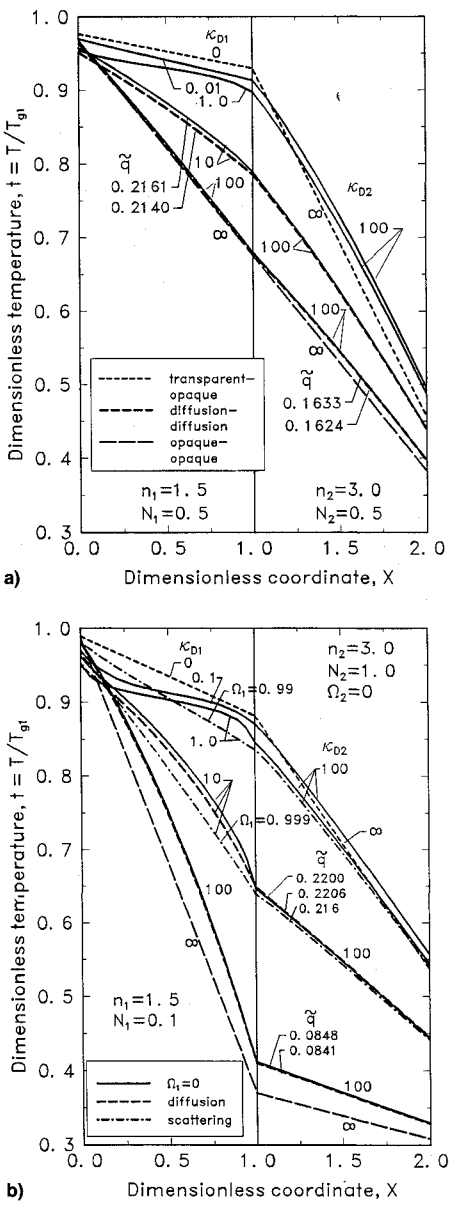


Fig. 6 Effect of having a second layer with a large optical thickness to simulate an opaque substrate; $t_{s1} = t_{g1} = 1$, $t_{s2} = t_{g2} = 0.25$, $H_1 = H_2 = 1$: a) equal thermal conductivity parameters in the two layers, and comparisons with three limiting cases and b) unequal thermal conductivity parameters in the two layers, $N_1 = 0.1$ and $N_2 = 1.0$, and results for high scattering in the first layer.

opaque (short dashes) and the opaque-opaque limits (long dashes), respectively. The diffusion-diffusion approximation, Eq. (18), is given (medium dashes) for the cases with large optical thicknesses in both layers; it provides a very good approximation for both temperature distribution and heat flux.

The thermal conductivities of the two layers are unequal in Fig. 6b, $N_1 = 0.1$ and $N_2 = 1.0$, compared with $N_1 = N_2 = 0.5$ in Fig. 6a. The temperature gradients are increased in the first layer and decreased in the second. Decreasing $N_1$ makes radiation more dominant so the temperature profiles in the first layer are less linear. The results approach the transparent-opaque (short dashes) and the opaque-opaque (long dashes) cases. For the large optical thicknesses comparisons are made with the diffusion-diffusion approximation, Eq. (18) (medium dashes), and very good predictions are obtained for temperatures and heat fluxes. For $\kappa_{D1} = 1$ and 10 the effect is shown of having high scattering in the first layer by letting $\Omega_1 = 0.99$ and 0.999, respectively, so the first layer retains the same absorption thickness, $(1 - \Omega_1)\kappa_{D1} = a_1 D_1 = 0.01$, for both high scattering cases. Since absorption in the first layer is small, the temperature profiles are dominated by heat conduction and they become nearly linear. The energy transfer through the first layer is not changed enough by the high $\Omega_1$ to appreciably modify the temperature distribution in the second layer.

The effect of large conduction in the second layer is in Fig. 7a where $N_2 = 10$; the $N_1 = 0.1$ remains the same as in Fig. 6b. The temperature profiles in the first layer have a larger range than Fig. 6b, temperature gradients in the second layer are smaller, and the heat flux is increased. Transparent-opaque (short dashes) and opaque-opaque results (long dashes) provide good limits, except near the outer surface of the first layer. For large optical thicknesses of both layers, the diffusion-diffusion solution (medium dashes) provides a very good estimate of the temperature distributions and the heat transfer.

The effect of increasing $\Omega_1$ is in Fig. 7b for the same parameters as Fig. 7a, and with $\Omega_1 = 0.99$ and 0.999. Increasing $\Omega_1$ makes the temperature profiles in the first layer more

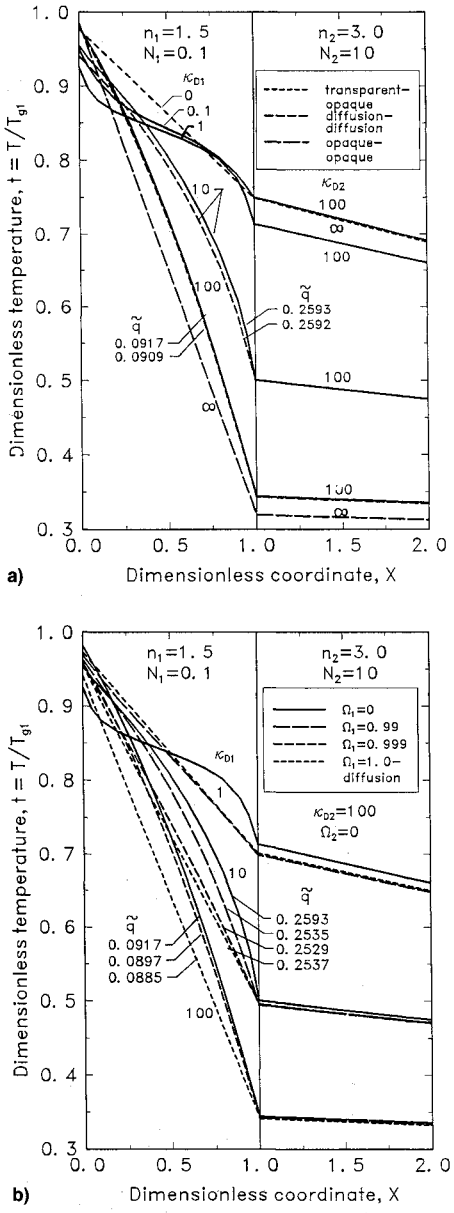


**Fig. 7 Effect of a high thermal conductivity parameter and optical thickness in the second layer; $t_{s1} = t_{g1} = 1$, $t_{s2} = t_{g2} = 0.25$, $H_1 = H_2 = 1$: a) optical thickness of the first layer in the range, $\kappa_{D1} = 0.01$–100 and b) effect of high scattering in the first layer, $\Omega_1 = 0.99$ and 0.999.**

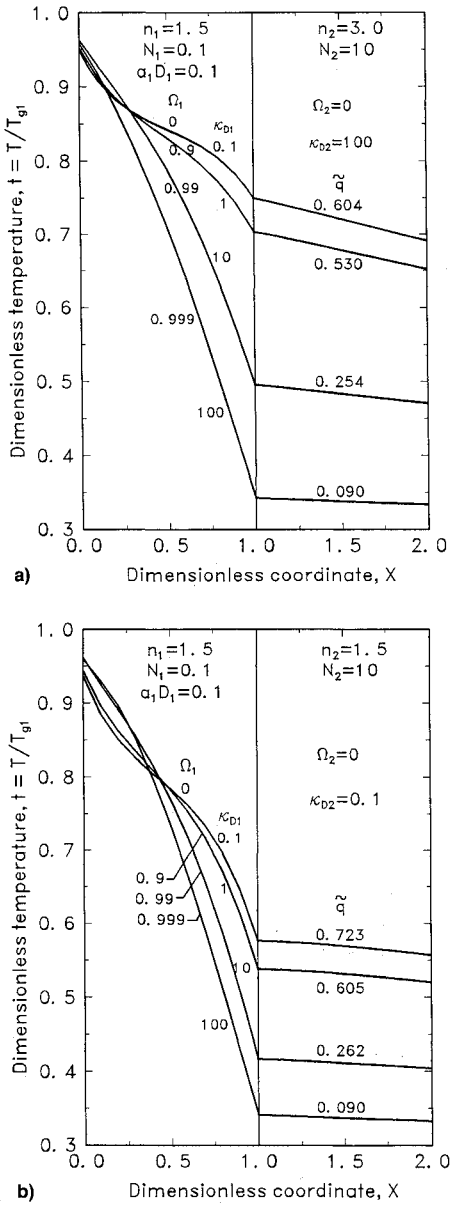


**Fig. 8 Effect of adding scattering while keeping absorption constant in the first layer, $a_1 D_1 = 0.1$; $t_{s1} = t_{g1} = 1$, $t_{s2} = t_{g2} = 0.25$, $H_1 = H_2 = 1$, $N_1 = 0.1$, $N_2 = 10$: a) $\kappa_{D2} = 100$, $n_1 = 1.5$, $n_2 = 3.0$ and b) $\kappa_{D2} = 0.1$, $n_1 = n_2 = 1.5$.**

linear as a result of decreased absorption and an increased effect of conduction. Comparisons are made with the limit of pure scattering in the first layer ($\Omega_1 = 1$) with diffusion in the second as calculated from Eq. (22) (short dash line). For large $\kappa_{D1}$, the temperature distributions for any $\Omega_1$ are nearly bounded by the limits of $\Omega_1 = 0$, pure absorption, and pure scattering, $\Omega_1 = 1$. In the limit of $\Omega_1 = 1$, there is a linear temperature distribution in the first layer since, without radiant absorption, the $t_1(X_1)$ depends only on heat conduction. Radiation is scattered through the first layer and absorbed by the second layer; this, along with heat conduction through the first layer, influences the level of the temperature distribution. The pure scattering-diffusion approximation (short dashes) predicts the heat fluxes and temperature distributions quite accurately for these high scattering cases with low absorption.

The effect of adding scattering to opacify the first layer is in Fig. 8a, where $a_1 D_1 = 0.1$ remains constant while the scattering is increased, so $\kappa_{D1}$ increases from 0.1 to 100. The second layer is optically thick, $\kappa_{D2} = 100$. Additional scattering reduces the energy transferred through the layers and decreases the temperature at the internal interface. In Fig. 8b the effect of an optically thin second layer is shown, $\kappa_{D2} = a_1 D_1 = 0.1$. Again, scattering is added to the first layer to increase its optical thickness. The refractive index of the two layers is the same to simulate a scattering layer combined with a nonscattering layer of the same material. The trends are similar to Fig. 8a.

## Conclusions

To investigate thermal behavior of a ceramic layer on a substrate, an analysis was developed and an iterative numerical technique used to solve the resulting system of interdependent equations for the temperature distribution and heat transfer. Limiting cases were developed for pure scattering in one layer, radiative diffusion in one or both layers, and one or both layers either transparent or opaque.

There are various interactions in a two-layer system that influence the temperature distribution and heat transfer. The refractive index of each layer significantly affects the temperature distribution in the laminate by producing internal reflections. Results were examined for refractive indices of 1.5 and 3, and optical thicknesses ranging from thin to thick. Increasing the refractive index of one layer makes the profile in that layer more uniform and changes the temperature level in the other layer. Near boundaries there can be large temperature gradients from the interaction of radiation and convection. Increasing scattering in the first layer while keeping its optical thickness constant makes its temperature profile more linear due to decreased absorption, and therefore, an increased effect of conduction. If scattering is added to opacify the first layer while keeping its absorption thickness constant, the temperature change in the first layer is substantially increased.

The limiting cases are readily evaluated and they provide accurate predictions for many useful ranges of parameters. The possible effect of scattering in the first layer can be determined by calculating the limits of pure absorption and pure scattering in that layer. For the latter case a special analytical solution was developed for the layer bonded to an optically thick second layer. The radiative diffusion approximation coupled with heat conduction gave very accurate predictions of temperatures and heat flows for optical thickness of each layer greater than about 10. When the optical thickness of each layer is larger than about 100, the temperatures approach the opaque limit.

## References


[1]Gardon, R., "Calculation of Temperature Distributions in Glass Plates Undergoing Heat-Treatment," *Journal of the American Ceramic Society*, Vol. 41, No. 6, 1958, pp. 200–209.

[2]Fowle, A. A., Strong, P. F., Comstock, D. F., and Sox, C., "Computer Program to Predict Heat Transfer Through Glass," *AIAA Journal*, Vol. 7, No. 3, 1969, pp. 478–483.

[3]Rokhsaz, F., and Dougherty, R. L., "Radiative Transfer Within a Finite Plane-Parallel Medium Exhibiting Fresnel Reflection at a Boundary," *Heat Transfer Phenomena in Radiation, Combustion and Fires*, American Society of Mechanical Engineers HTD-Vol. 106, 1989, pp. 1–8.

[4]Ping, T. H., and Lallemand, M., "Transient Radiative-Conductive Heat Transfer in Flat Glasses Submitted to Temperature, Flux, and Mixed Boundary Conditions," *International Journal of Heat and Mass Transfer*, Vol. 32, No. 5, 1989, pp. 795–810.

[5]Crosbie, A. L., and Shieh, S. M., "Three-Dimensional Radiative Transfer for Anisotropic Scattering Medium with Refractive Index Greater than Unity," *Journal of Quantitative Spectroscopy and Radiative Transfer*, Vol. 44, No. 2, 1990, pp. 299–312.

[6]Viskanta, R., and Grosh, R. J., "Heat Transfer by Simultaneous Conduction and Radiation in an Absorbing Medium," *Journal of Heat Transfer*, Vol. 84, No. 1, 1962, pp. 63–72.

[7]Amlin, D. W., and Korpela, S. A., "Influence of Thermal Radiation on the Temperature Distribution in a Semi-Transparent Solid," *Journal of Heat Transfer*, Vol. 101, No. 1, 1979, pp. 76–80.

[8]Spuckler, C. M., and Siegel, R., "Refractive Index Effects on Radiative Behavior of a Heated Absorbing-Emitting Layer," *Journal of Thermophysics and Heat Transfer*, Vol. 6, No. 4, 1992, pp. 596–604.

[9]Spuckler, C. M., and Siegel, R., "Refractive Index and Scattering Effects on Radiative Behavior of a Semitransparent Layer," *Journal of Thermophysics and Heat Transfer*, Vol. 7, No. 2, 1993, pp. 302–310.

[10]Siegel, R., and Spuckler, C. M., "Effect of Index of Refraction on Radiation Characteristics in a Heated Absorbing, Emitting and Scattering Layer," *Journal of Heat Transfer*, Vol. 114, No. 3, 1992, pp. 781–784.

[11]Tarshis, L. A., O'Hara, S., and Viskanta, R., "Heat Transfer by Simultaneous Conduction and Radiation for Two Absorbing Media in Intimate Contact," *International Journal of Heat and Mass Transfer*, Vol. 12, No. 3, 1969, pp. 333–347.

[12]Siegel, R., and Spuckler, C. M., "Refractive Index Effects on Radiation in an Absorbing, Emitting and Scattering Laminated Layer," *Journal of Heat Transfer*, Vol. 115, No. 1, 1993, pp. 194–200.

[13]Anderson, E. E., and Viskanta, R., "Spectral and Boundary Effects on Coupled Conduction-Radiation Heat Transfer Through Semitransparent Solids," Wärme- and Stoffübertragung, Vol. 6, No. 1, 1973, pp. 14–24.

[14]Thomas, J. R., Jr., "Coupled Radiation/Conduction Heat Transfer in Ceramic Liners for Diesel Engines," *Numerical Heat Transfer*, Pt. A, Vol. 21, No. 1, 1992, pp. 109–120.

[15]Siegel, R., and Howell, J. R., *Thermal Radiation Heat Transfer*, 3rd ed., Hemisphere, Washington, DC, 1992.

[16]Cox, R. L., "Fundamentals of Thermal Radiation in Ceramic Materials," *Thermal Radiation in Solids*, edited by S. Katzoff, NASA SP-55, 1965, pp. 83–101.

[17]Richmond, J. C., "Relation of Emittance to Other Optical Properties," *Journal of Research of the National Bureau of Standards*, Vol. 67C, No. 3, 1963, pp. 217–226.

[18]Howell, J. R., and Goldstein, M. E., "Effective Slip Coefficients for Coupled Conduction-Radiation Problems," *Journal of Heat Transfer*, Vol. 91, No. 1, 1969, pp. 165, 166.

[19]Heaslet, M. A., and Warming, R. F., "Radiative Transport and Wall Temperature Slip in an Absorbing Planar Medium," *International Journal of Heat and Mass Transfer*, Vol. 8, No. 7, 1965, pp. 979–994.